IEEE Access
Multidisciplinary | Rapid Review | Open Access Journal

Received August 11, 2020, accepted August 24, 2020, date of publication August 27, 2020, date of current version September 10, 2020.

Digital Object Identifier 10.1109/ACCESS.2020.3019820

System Design of Gigabit HAPS Mobile Communications

YOHEI SHIBATA[1,2], NOBORU KANAZAWA[1], MITSUKUNI KONISHI[1,2], KENJI HOSHINO[1,2], YOSHICHIKA OHTA[1,2], AND ATSUSHI NAGATE[1,2], (Member, IEEE)

[1]SoftBank Corporation, Tokyo 135-0064, Japan
[2]HAPSMobile Inc., Tokyo 135-0064, Japan

Corresponding author: Yohei Shibata (yohei.shibata02@g.softbank.co.jp)

ABSTRACT High-altitude platform stations (HAPSs) are expected to provide ultrawide-coverage areas and disaster-resilient networks from the stratosphere at around 20 km by installing wireless equipment on HAPS. Because their altitude is much lower than that of communications satellites, HAPSs can provide mobile communications services directly to smartphones, which are commonly used in terrestrial networks, such as fourth generation Long Term Evolution. Considering the widespread nature of mobile broadband communications and the importance as a backup line in case of disaster, HAPSs are expected to provide a large capacity in the future. A cellular system with single-cell frequency reuse using multiple cells similar to terrestrial mobile communications should be introduced to achieve such a capacity. The number of cells that a HAPS can accommodate ranges from 1 to more than 100, depending on unmanned aerial vehicle (UAV) ability. By contrast, the optimal cell configuration, which depends on the number of available cells, has not been clarified in previous research. In this paper, we propose an optimization method for the cell configuration for HAPS mobile communications using a genetic algorithm, which can be generally applied regardless of the number of cells and can clarify the optimal cell configuration. Although many cells are required to achieve gigabit-class HAPS mobile communications, the heightened power consumption due to the large number of cells is a critical problem for UAVs. Thus, we also investigate the reduction of the total transmission power and demonstrate the feasibility of energy-efficient gigabit HAPS mobile communications with wide coverage.

INDEX TERMS Cell configuration, energy efficiency, genetic algorithms, HAPS, optimization.

I. INTRODUCTION

For the realization of ultra-wide coverage and disaster-resilient networks, a high-altitude platform station (HAPS) offers great potential for innovation in the field of mobile communications [1]. HAPS mobile communications use unmanned aerial vehicles (UAVs), such as balloons, airships, and other aircraft, that fly in the stratosphere at an altitude of 20 km, where low wind speeds are expected. Although HAPSs are mainly expected to provide fixed communications infrastructure for Internet backhaul, they also have potential for mobile communications that use the same systems as those of terrestrial networks, such as fourth generation Long Term Evolution (4G LTE) and fifth generation New Radio (5G NR) [2]–[5]. Because the altitude of HAPSs is significantly lower than that of communications satellites, e.g., 36,000 km for stationary satellites, a HAPS can provide mobile communications services directly to smartphones, which are commonly used in terrestrial mobile communications networks with 4G LTE and, eventually 5G NR. HAPSs can provide disaster-resilient mobile communications services; users can communicate immediately during a disaster without reliance on special equipment, such as satellite communications terminals.

Although HAPS mobile communications has been studied since the 1990s [2], it is still not at the commercialization stage. However, the technology has been gaining considerable attention recently due to significant improvements in UAV technology. For example, Airbus succeeded in an almost-one-month flight with its solar-powered UAV, the Zephyr S, in 2018 [6], and Alphabet's Loon completed a 100-day flight with its balloon-type UAV and launched a commercial service in 2020 [7], [8]. Furthermore, HAPSMobile Inc. is attempting to provide mobile communications services from the sky and developing a solar-powered UAV named Sunglider [9].

The associate editor coordinating the review of this manuscript and approving it for publication was Jie Tang.

HAPS mobile communications are expected to cover very wide areas, including those that are currently out of service under terrestrial mobile communications. They are also expected to cover aerial areas in a three-dimensional fashion to give drones and other flying vehicles stable control and data communications links in the future. Considering the widespread nature of mobile broadband communications and the particularly rapid increase in traffic during disasters, HAPSs require a very large capacity, which necessitates a multi-cell configuration with single-cell frequency reuse (much like terrestrial mobile communications); this configuration is also essential for realizing wide coverage areas. By dividing a coverage area into multiple cells, each cell can have a narrow beamwidth, which improves the antenna gain and link budget, thereby widening the coverage area. Additionally, with single-cell frequency reuse, the total capacity of HAPSs improves with the number of cells, as is observed in terrestrial mobile communications.

Various studies related to HAPS mobile communications have been conducted [10]–[14]. For example, some studies focused on antenna optimization for specific cell configurations [10], [11], whereas others evaluated communications quality with cellular systems such as 4G LTE and WiMAX [12]–[14]. However, detailed studies on various cell configuration types depending on the number of available cells, such as those aiming to optimize the antenna patterns and tilt angles by considering the required communications quality, have not been conducted in conventional research.

In this paper, we propose a cell configuration optimization method with an arbitrary number of cells for HAPS mobile communications [5]. We first define an antenna pattern model and cell configurations for optimization. The number of parameters required to form a cell configuration increases as a cell configuration becomes complex. Given the large combination of multiple parameters, finding optimal parameters with exhaustive search is difficult. Thus, we use a genetic algorithm (GA) to identify the optimal combination in a practical time. Cell configuration optimization with GA is effective because the number of cells a HAPS can accommodate ranges from 1 to more than 100, depending on UAV ability. We then clarify which cell configuration is optimal in terms of spectral efficiency under the constraints of communications quality. Finally, we identify the cell configuration that is suitable for achieving gigabit-class HAPS mobile communications.

Although capacity can be enhanced by increasing the number of cells, the installation of many cells on a UAV is normally restricted by the acceptable payload mass and power consumption [15]. For example, airships and solar airplanes have maximum weights of 1000–2000 kg and 5–300 kg, respectively. Similarly, the maximum supported power consumptions of airships and solar airplanes are 10 kW and 100–3000 W, respectively [1], [8]. Therefore, energy efficiency, including transmission power reduction, should be considered to decrease power consumption. This would lead to fewer batteries and solar panels, thereby improving UAV performance. In this paper, we also investigate reducing the transmission power to reduce the overall power consumption of HAPSs, and we clarify the relationship among power consumption, coverage, and throughput performance.

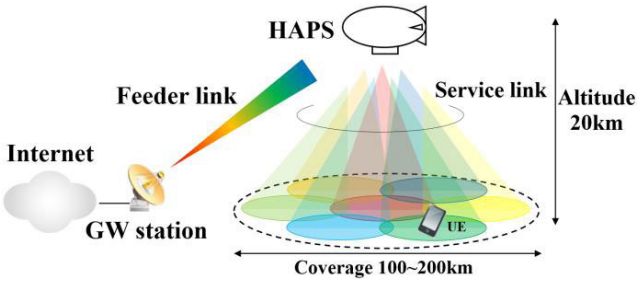

FIGURE 1. HAPS system configuration.

The rest of this paper is organized as follows. Section II describes the concept of HAPS mobile communications. The problem formulation and system design, including the definition of cell configurations, antenna pattern, and application of the GA are presented in Section III. Evaluation results are presented in Section IV, and the concluding remarks are given in Section V.

II. BASIC CONCEPT OF HAPS SYSTEM

Fig. 1 illustrates an example of a HAPS mobile communications system configuration. HAPSs provide mobile communication services through two schemes: one has base stations on HAPSs and the other relays signals from a base station on the ground; in this paper, we define them as BS and repeater types, respectively.

For the repeater type, base stations (evolved node B [eNB]) are connected to an Evolved Packet Core (EPC) and placed at a gateway (GW) station. The signals from the base station are transmitted from the GW station through a feeder link and relayed at the repeater on the HAPS in a non-regenerative fashion. This relayed signal is then directly transmitted to mobile terminals, such as smartphones, through a service link. By contrast, the BS type places base stations on the HAPS, and they are connected to an EPC by Fixed Wireless Access (FWA) as a backhaul between the GW station and the HAPS. The signals from the base station are transmitted to mobile terminals directly.

HAPS communications use high frequencies, such as 6.5 GHz, 28 GHz, and 47 GHz for feeder links; it uses 2 GHz for service links, which is the same frequency used for terrestrial mobile communications services [16]. Thus, ordinary smartphones can be used with HAPS mobile communications without modification. Extending frequency bands was discussed in the World Radiocommunication Conference 2019 (WRC-19) [17], and new bands, such as 24.25-27.5GHz, 37-43.5GHz, and 66-71GHz were identified as new global bands.

Fig. 1 demonstrates a case of seven cells in a service link with single-cell frequency reuse. For example, 10 MHz LTE communications require 10 MHz for each downlink (DL) and uplink (UL) in the service link for both BS and repeater types

TABLE 1. Parameters for cell configurations.

Parameters	1 layer	2 layers		3 layers	
	(0, N) config.	(M, $N-M$) config. M=1	(M, $N-M$) config. $M\neq 1$	(1, M, $N-M-1$) config.	(3, M, $N-M-3$) config.
Vertical beamwidth	$\theta_{3\mathrm{dB,1layer}}$	$\theta_{3\mathrm{dB,2layer}}$	$\theta_{3\mathrm{dB,1layer}}$ $\theta_{3\mathrm{dB,2layer}}$	$\theta_{3\mathrm{dB,2layer}}$ $\theta_{3\mathrm{dB,3layer}}$	$\theta_{3\mathrm{dB,1layer}}$ $\theta_{3\mathrm{dB,2layer}}$ $\theta_{3\mathrm{dB,3layer}}$
Beamwidth (central cell) (vertical, horizontal)	-	$\theta_{3\mathrm{dB,ctr}}$	-	$\theta_{3\mathrm{dB,ctr}}$	-
Antenna tilt angle	$\theta_{\mathrm{tilt,1layer}}$	$\theta_{\mathrm{tilt,2layer}}$	$\theta_{\mathrm{tilt,1layer}}$ $\theta_{\mathrm{tilt,2layer}}$	$\theta_{\mathrm{tilt,2layer}}$ $\theta_{\mathrm{tilt,3layer}}$	$\theta_{\mathrm{tilt,1layer}}$ $\theta_{\mathrm{tilt,2layer}}$ $\theta_{\mathrm{tilt,3layer}}$
Horizontal beamwidth	$\phi_{3\mathrm{dB,1layer}}$	$\phi_{3\mathrm{dB,2layer}}$	$\phi_{3\mathrm{dB,1layer}}$ $\phi_{3\mathrm{dB,2layer}}$	$\phi_{3\mathrm{dB,2layer}}$ $\phi_{3\mathrm{dB,3layer}}$	$\phi_{3\mathrm{dB,1layer}}$ $\phi_{3\mathrm{dB,2layer}}$ $\phi_{3\mathrm{dB,3layer}}$
Layer rotation	ω	$\omega_{2\mathrm{layer}}$	$\omega_{1\mathrm{layer}}$ $\omega_{2\mathrm{layer}}$	$\omega_{2\mathrm{layer}}$ $\omega_{3\mathrm{layer}}$	$\omega_{1\mathrm{layer}}$ $\omega_{2\mathrm{layer}}$ $\omega_{3\mathrm{layer}}$

because single-cell frequency reuse is applied. The feeder link requires 70 MHz for each DL and UL because seven 10 MHz spectrum cells must be aggregated for the repeater-type. The bandwidth of the feeder link for the BS type can be reduced depending on the efficiency of the FWA.

Cell movement and deformation, which are caused by changes in antenna direction as a result of UAV movement and vibration during flight, must be considered in HAPS communications. Variations in movement can lead to many handovers, which increase unnecessary control signals and degrade communications quality. A beamforming technique and a necessary antenna configuration that fixes cell locations regardless of UAV movement were studied to avoid this issue [4]. Such research showed that beamforming can control beam direction to offset UAV movement; thus, cell location remains the same regardless of the UAV's position. In this paper, we assume that cell locations remain the same regardless of UAV movement owing to the use of this beamforming technique.

III. SYSTEM DESIGN

In this section, we describe the system design of HAPS mobile communications. First, the cell configurations to be optimized are defined, and an antenna pattern is modeled. Then, coverage constraints are explained. Finally, we present a cell configuration optimization method that uses a GA. This method can be applied regardless of the number of cells. Cell configurations are optimized to maximize throughput under the coverage constraints. Finding an optimal result through an exhaustive search is difficult because the cell configuration becomes complex as the number of cells increases. Therefore, GA can be an optimization solution because it provides a good solution in a practical time.

A. CELL CONFIGURATION

For a given number of cells, there could be several possible cell configurations. For example, Fig. 2 shows cell configurations when the number of cells, N, is 9. Thus, we define cell configurations to be optimized to clarify optimal cell configurations.

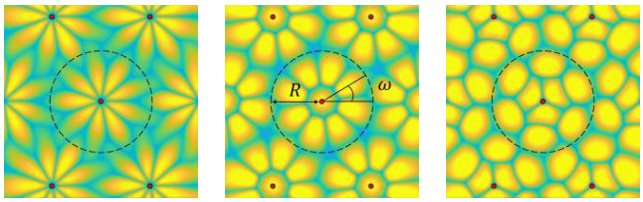

(a) (0, N) config. (b) (1, N-1) config. (c) (3, N-3) config.

FIGURE 2. Example of cell configuration ($N = 9$).

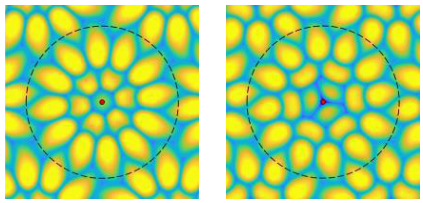

(a) N=19, (1,6,12) (b) N=21, (3,6,12)

FIGURE 3. Example of three-layer cell configuration.

Because signals are emitted from the HAPS radially, circular layered cell configurations are desirable. First, one and two-layer configurations are defined in Fig. 2. Fig. 2(a) depicts a one-layer configuration that is the same as that of a multi-sector base station for terrestrial networks; this is defined as the $(0, N)$ configuration. Figs. 2(b) and 2(c) are two-layer configurations; their first layers have one and three cells, respectively. They are defined as the $(M, N-M)$ configuration, where M is either 1 or 3. The three-layer configuration in Fig. 3 is defined for large numbers of cells, e.g., 19 and 21 cells. Figs. 3(a) and 3(b) are defined as the $(1, M, N-M-1)$ and $(3, M, N-M-3)$ configurations, respectively. Fig. 3 shows a case when M is 6. As this is a three-layer configuration, we consider cases when M is 5, 6, and 7 in this paper.

As can be seen in Table 1, the parameters required to form a cell are as follows: vertical half-power beamwidth, $\theta_{3\mathrm{dB}}$; horizontal half-power beamwidth, $\phi_{3\mathrm{dB}}$; antenna tilt angle, θ_{tilt}; and layer rotation, ω, as shown in Fig. 2 (b). The layer rotation is the horizontal-pointing direction of a layer, and $\omega = 0$ is defined as a case when a surrounding cell is immediately

to the right of the center point. The layer rotation, ω, should be optimized because throughput is affected by interference from other HAPSs or other layers, depending on its rotation. The $(0, N)$ configuration requires these four parameters. In addition to these parameters, the half-power beamwidth for the central cell, $\theta_{3\mathrm{dB,ctr}}$, is required for the $(1, N-1)$ and $(1, M, N-M-1)$ configurations because there is a cell just beneath the HAPS. The $(M, N-M)$ configuration, where $M \neq 1$, and the $(3, M, N-M-3)$ configuration can be regarded as a combination of $(0, N)$ configurations for each layer. Thus, the $(M, N-M)$ configuration requires eight parameters, which is double that of the $(0, N)$ configuration; the $(3, M, N-M-3)$ configuration requires 12 parameters, which is triple that of the $(0, N)$ configuration. The combination of parameters becomes large as the cell configuration becomes complex, making optimization difficult.

B. ANTENNA PATTERN

In this paper, we define an antenna pattern to approximate a planar patch array antenna, which is modified from International Telecommunication Union Radiocommunication Sector (ITU-R) recommendations [16]. Although the antenna pattern in [16] assumes parabolic antennas, where the vertical and horizontal beamwidths are the same, we need to calculate the antenna gains for the vertical and horizontal planes separately because we assume using a planar patch antenna. Thus, the antenna gains are calculated for the vertical and horizontal planes separately, and they are then combined. The antenna gains for the angle Ψ can be written as:

$$G(\Psi) = \begin{cases} -3\,(\Psi/\Psi_b)^2\,; & 0 \le \Psi \le \Psi_1 \\ L_N\,; & \Psi_1 < \Psi \le \Psi_2 \\ X - A\log_{10}(\Psi); & \Psi_2 < \Psi \le \Psi_3 \\ L_F\,; & \Psi_3 < \Psi \end{cases} \quad (1)$$

where Ψ_b is the half-power beamwidth, $\Psi_1 = \Psi_b\sqrt{-L_N/3}$, $\Psi_2 = 3.745\Psi_b$, $X = L_N + A\log_{10}(\Psi_2)$, and $\Psi_3 = 10^{(X-L_F)/10}$. On the basis of a real antenna pattern that can be realized for a planar patch array antenna, we modified the near-in-side-lobe level, L_N; far side-lobe level, L_F; and A to -20 dB, -30 dB, and 20, respectively. Thus, the antenna gain can be expressed as

$$G = \max\left(G_v + G_h, L_F\right) + G_p \quad (2)$$

where G_v and G_h are the vertical and horizontal antenna gains, respectively, as calculated in Eqn. 1. Then the maximum antenna gain G_p is expressed as

$$G_p = 10\log_{10}\left(\frac{80^2}{\theta_{3\mathrm{dB}}\phi_{3\mathrm{dB}}}\right) + 6, \quad (3)$$

which is based on an antenna with a 6 dBi gain and a beamwidth of 80° for both the vertical and horizontal planes. Fig. 4 shows an example of an antenna pattern.

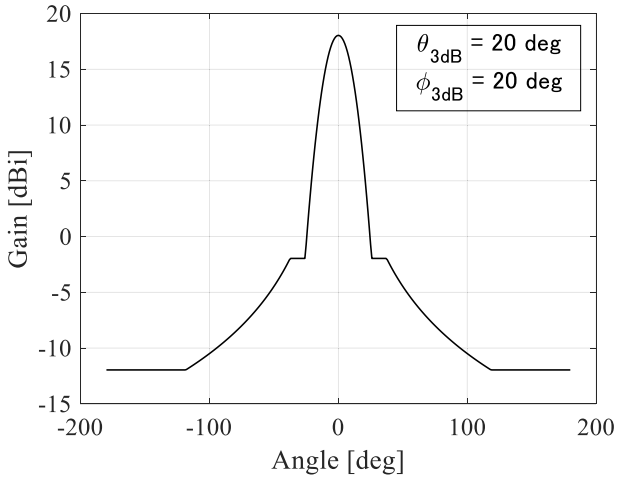

FIGURE 4. Example of antenna pattern for V or H polarization.

C. COVERAGE CONDITIONS

Cell configurations are optimized while maximizing throughput under coverage conditions. In this paper, coverage conditions are defined by the signal-to-noise ratio (SNR) for both DL and UL and by the signal-to-noise-plus-interference ratio (SINR) for DL. Specifically, 99% of all users should satisfy the following constraints:

- DL SNR above 8 dB,
- UL SNR above 11 dB, and
- DL SINR above -7 dB when all HAPSs transmit signals at maximum power (full buffer).

These SNR constraints are defined based on the required SNR, which is based on our measurement, for which we assume 2×2 multiple-input, multiple-output (MIMO) for DL and 1×2 single-input, multiple-output (SIMO) for UL.

For the DL SNR, the constraint is defined based on a minimum SNR of -7 dB, which can achieve a Block Error Rate (BLER) of less than 10% with minimum Modulation and Coding Scheme (MCS). The MCS is a combination of the modulation scheme and coding rate. The higher the MCS, the more bits can be transmitted per time unit. We assume a 15 dB link margin to -7 dB SNR to consider loss factors, such as body loss and indoor penetration loss, although our simulation assumes free-space path loss.

For UL, -4 dB is the minimum SNR to be connected under the condition that realizes transport block size required to transmit at least radio resource control messages; that is, the number of resource blocks (RBs) is two, and that of MCS is three. As with the DL SNR, we assume a 15 dB link margin to the minimum UL SNR.

The DL SINR constraint is also based on our measurement. We focus only on the DL SINR rather than the UL SINR because we assume DL traffic is dominant compared to UL traffic in this paper.

Coordinated multi-point (CoMP) reception, which is used in mobile wireless communications systems such as 4G LTE, can be a good solution for extending the coverage area for the UL [19]. The UL CoMP allows us to obtain the diversity

TABLE 2. System parameters.

Parameters	Downlink	Uplink
Frequency	2 GHz	
Antenna configuration	2 × 2 MIMO	1 × 2 SIMO
Transmitter		
Transmission power	Design parameter	23 dBm/antenna
Bandwidth	18 MHz	360 kHz
Antenna gain	Design parameter	−3 dBi
Propagation	Free space loss	
Receiver		
Antenna gain	−3 dBi	Design parameter
Noise figure	5 dB	3 dB
Required SNR (including margins)	8 dB	11 dB

gain by receiving signals from user equipment (UE) in several neighboring cells, making it possible to improve the UL SNR, especially at cell borders, and extend the coverage area. Furthermore, CoMP can narrow the beamwidth to meet the UL SNR constraint, assuming the same coverage area. At the same time, a narrower beam can reduce DL interference with other cells, thus improving the DL SINR and throughput. In this study, we clarify the effectiveness of UL CoMP. We perform UL CoMP between two cells where the UE-received power at the base stations is the highest. Although the receiver diversity is expected to be with four antennas of two cells, we assume polarization diversity. Thus, receiver diversity will effectively be with two antennas (one antenna for each cell). Assuming maximum ratio combining with two receiver antennas, we calculate the UL SNR. CoMP is performed for cells belonging to the same HAPS; CoMP between cells from different HAPS systems is not assumed.

Table 2 lists major system parameters. We use a 2 GHz frequency, which is a HAPS mobile communications service band in ITU-R [16]. The DL antenna configuration is 2 × 2 MIMO. We set the bandwidth to 18 MHz, which is the largest LTE system bandwidth. The antenna gain, which is defined in Eqn. 3, is optimized based on the evaluation parameters. Note that the antenna gain can be improved by increasing the number of cells, thus narrowing the beamwidth, and creating room to reduce the DL transmission power. The propagation model assumes free space loss due to the good line-of-sight environment. The UE antenna gain, G_{UE}, is assumed to be −3 dBi, in accordance with [18]. The noise figure is assumed to be 5 dB for UE and 3 dB for the base station, which correspond to typical commercial device and base station implementations. For the UL, we assume receiver diversity with a one-transmission-antenna and two-reception-antenna configuration (polarization diversity). The UL bandwidth is 360 kHz, which corresponds to 2 RBs and is required to achieve UL connection. The UE transmission power is 23 dBm, which is typical for LTE UE.

Based on the above explanation, we describe SINR and SNR calculation. DL received signal level for u-th UE from c-th cell of h-th HAPS in dB is calculated as

$$R_{u,c,h} = P_t + G_{u,c,h} - L_{u,h} + G_{UE} \tag{4}$$

where P_t is a BS transmission power, $G_{u,c,h}$ is the BS antenna gain of c-th cell in h-th HAPS for u-th UE which is based on Eqn. 2 and $L_{u,h}$ is the free-space path loss between u-th UE and h-th HAPS, which is calculated by

$$L_{u,h} = 20\log_{10}\left(\frac{4\pi r_{u,h}}{\lambda}\right) \tag{5}$$

where $r_{u,h}$ is the distance between u-th UE and h-th HAPS and λ is the wavelength. For the u-th UE, $N_{HAPS} \times N$ values are calculated, where N_{HAPS} is the number of HAPSs and N is the number of cells in a HAPS. The cell, to which u-th UE connects is defined as a cell with the highest received level among $N_{HAPS} \times N$ cells. Let c_u and h_u a cell and HAPS index to which u-th UE connects. Total interference power of u-th UE which is connected to c_u-th cell of h_u-th HAPS in dB is calculated by

$$I_u = 10\log_{10}\left(\beta\left\{\sum_{j=1,j\neq c_u}^{N} 10^{\left(\frac{R_{u,j,h_u}}{10}\right)} + \sum_{i=1,i\neq h_u}^{N_{HAPS}}\sum_{j=1}^{N} 10^{\left(\frac{R_{u,j,i}}{10}\right)}\right\}\right) \tag{6}$$

where $\beta \in [0, 1]$ is an activation factor representing how much RBs are used in adjacent cells. Note that $i = 1$ represents the central HAPS.

The DL SNR and DL SINR of u-th UE which is connected to c_u-th cell of h_u-th HAPS in dB is then represented as

$$\gamma_{SNR,u} = 10\log_{10}\left(\frac{10^{\frac{R_{u,c_u,h_u}}{10}}}{\sigma^2}\right) \tag{7}$$

and

$$\gamma_{SINR,u} = 10\log_{10}\left(\frac{10^{\frac{R_{u,c_u,h_u}}{10}}}{\sigma^2 + 10^{\frac{I_u}{10}}}\right) \tag{8}$$

where σ^2 is the noise power. The noise power in dB is calculated as

$$\sigma^2_{dBm} = -174 + 10\log(BW) + NF \tag{9}$$

where BW is the bandwidth and NF is noise figure. Because we focus on the central HAPS, we consider DL SNR and DL SNR when $h_u = 1$ in the evaluation. Similarly, the UL received signal level of u-th UE in c-th cell of h-th HAPS is calculated as

$$R'_{u,c,h} = P'_t + G_{UE} - L_{u,h} + G_{u,c,h} \tag{10}$$

TABLE 3. Parameter range for optimization.

Parameters	Search range
Vertical beamwidth	$0° < \theta_{3dB} < 90°$
Beamwidth for central cell	$0° < \theta_{3dB,ctr} < 180°$
Antenna tilt angle	$\tan^{-1}(h/R) < \theta_{tilt} < 90°$
Horizontal beamwidth	$0° < \phi_{3dB} < 360°/n$
Layer rotaion	$0° < \omega < 360°/n$

Note: n is the number of cells in a layer to focus on and h, R are HAPS height (20 km) and area radius.

where P'_t is the UE transmission power. The cell and HAPS to which a UE connects is determined by the DL received level, that is, the cell with maximum DL received power, which is denoted as c_u and h_u. When the second strongest signal power from u-th UE in the h_u-th HAPS is denoted as R'_{u,c_u',h_u} where $c'_u \neq c_u$, UL SNR is calculated assuming UL CoMP as

$$\gamma'_{SNR,u} = 10\log_{10}\left(\frac{10^{\frac{R'_{u,c_u,h_u}}{10}} + 10^{\frac{R'_{u,c_u',h_u}}{10}}}{\sigma^2}\right) \quad (11)$$

Similar to DL, UL SNR for the central HAPS is considered in the evaluation.

D. OPTIMIZATION OF CELL CONFIGURATION AND PROBLEM FORMULATION

As stated in Section III-A, the combination of multiple antenna parameters enlarges as the cell configuration becomes complex. Thus, we optimize the combination using a GA, an optimization algorithm that is inspired by natural selection and provides high-quality solutions in a practical time. In GA, a population of candidate solution called individuals goes through operations inspired by processes, such as crossover and mutation toward better solutions.

First, individuals are defined as a combination of parameter index for each parameter to be optimized. A vector for an individual is represented as $\boldsymbol{p} = [p_1, p_2, \cdots, p_K]$, where K is the number of parameters and different according to the cell configuration, as explained in Section III-A. For example, K is 4 for the $(0, N)$ configuration, 5 for the $(1, N-1)$ configuration and 8 for the $(M, N-M)$ configuration where $M \neq 1$. The k-th parameter index p_k, $1 \leq k \leq K$ takes a positive integer value where the maximum value is the number of candidates for each parameter. The search range for the parameters during the optimization process is defined in Table 3 and takes a value every 2°. The lower limit of the antenna tilt angle, θ_{tilt}, is set to orient the antenna direction toward the inside of the HAPS coverage area. For example, the range for vertical beamwidth is $0^\circ < \theta_{3\text{dB}} \leq 90^\circ$ according to Table 3, Thus, p_k for vertical beamwidth takes the value between 1 and 45 when the step size is 2°, which corresponds to 2° to 90°. When the total number of combinations is represented as J, the pool of possible parameters available is denoted as $\mathcal{P} : \{\boldsymbol{p}^1, \boldsymbol{p}^2, \cdots, \boldsymbol{p}^J\}$, where $\boldsymbol{p}^j$, $1 \leq j \leq J$, is j-th individual.

Next, an initial population, which is a group of individuals is created randomly where the population size (popsize) is 50 for $K \leq 5$ and 200 for otherwise. Then fitness value is calculated for every individual in the population based on the DL spectral efficiency. The u-th UE's DL spectral efficiency, which is based on the Shannon capacity, can be expressed as

$$C_u = M\alpha\frac{N_{\text{avg}}}{N_{c_u}}\log_2\left(1 + \gamma_{SINR,u}\right) \quad (12)$$

In the above equation, M, α, N_{avg}, N_{c_u}, and $\gamma_{SINR,u}$ stand for the number of antennas, transmission efficiency, the number of average users among the cells in the HAPS, the number of users in the c_u-th cell, and SINR of the u-th user in the c_u-th cell of the central HAPS which is based on Eqn. 8, respectively. Note that the index for HAPS is omitted because we focus only on the central HAPS. In this case, M has a value of 2 because we assume 2×2 MIMO antennas and α is set to 0.5, which is the typical LTE implementation value for reflecting overhead, such as cyclic prefix, guard intervals and control channels.

We define a set of the DL spectral efficiency, C_u, for all UEs in the central HAPS as $\mathbb{C}$. The goal is to maximize the 50th percentile value (median value) of the spectral efficiency of users connected to the central HAPS $\mathbb{C}$, which can formally be written as

$$\begin{aligned} &\max_{\boldsymbol{P}} \text{median}(\mathbb{C}) \\ &\text{s.t. } \boldsymbol{P} \in \mathcal{P} \\ &\quad DLSNR_{1\%} > 8\,\text{dB} \\ &\quad ULSNR_{1\%} > 11\,\text{dB} \\ &\quad DLSINR_{1\%} > -7\,\text{dB} \end{aligned} \quad (13)$$

where $DLSNR_{1\%}$, $ULSNR_{1\%}$ and $DLSINR_{1\%}$ are the 1st percentile values of the DL SNR, UL SNR, and DL SINR of the connected users to the central HAPS. Note that $DLSINR_{1\%}$ is calculated assuming full buffer, that is, $\beta = 1$ in Eqn. 6.

Eqn. 12 is deemed to have weighted capacity because of the factor N_{avg}/N_{c_u}. Depending on the antenna design, the cell size varies even within a given HAPS area. The effective throughput will decrease in this case because users in smaller areas have a higher probability of obtaining radio resource allocation, whereas users in larger areas have a lower probability. The term N_{avg}/N_{c_u} is effective for avoiding the throughput decrease that results from disparities in the number of users for each cell. For example, if N_{avg}/N_{c_u} becomes less than 1, the capacity of users in the c_u-th cell will decrease uniformly because the limited resource is then shared with more users. Therefore, Eqn. 12 is effective in terms of the total HAPS capacity because some users are offloaded to other cells to maximize the total capacity of the HAPS.

After calculating fitness value based on Eqn. 12 for all individuals in the population, the best 5% of the population

is preserved as elite offspring for the next generation. The 80% of the new population of the next generation is produced by uniform crossover where each element in an individual is randomly copied from the first or from the second parent. The parents are randomly selected based on roulette wheel selection (RWS), which is commonly used for GAs and the fitness value is modified in a way to consider violation of constraint functions based on [20]: If the individual is feasible, the calculated fitness value is used and if the individual is infeasible, the fitness value is changed to the maximum fitness value among feasible individuals of the population, plus a sum of the constraint violations of the (infeasible) point. Furthermore, the fitness value is scaled so that it is suitable for selection of RWS removing the effect of the spread of the raw fitness value. The raw fitness value is scaled based on the rank of each individual instead of its score, which means the assigned values depends only on an individual's rank. The rank of an individual is its position in the sorted scores: the rank of the most fit individual is 1, the next most fit is 2, and so on. The scaled fitness value with rank n is proportional to $1/\sqrt{n}$. The probability of an individual to be chosen as a parent is proportional to its scaled fitness value. The remaining 15% of a generation comes from random mutation which consists of two steps: First the algorithm selects individuals for mutation randomly. In the second step, each element in an individual is replaced by random value with the probability of 0.01. This process of producing new generation continues to make better solutions and termination occurs when stopping criteria is satisfied, that is, the best median value of objective function results remains unchanged for 50 generations.

IV. EVALUATION

A. EVALUATION CONDITIONS

In this paper, we evaluate HAPS mobile communications with 7, 9, 12, 19, and 21 cells. We assume a continuous coverage area covered by deploying multiple HAPSs on a hexagonal grid, as displayed in Fig. 2. The number of HAPSs is 7, and $7N$ cells (7 HAPSs $\times$ N cells) in total are considered in our evaluation to consider interference. When the radius of the HAPS coverage area is denoted as R km, as in Fig. 2, each HAPS is located $R\sqrt{3}$ km apart on the hexagonal grid. In the evaluation, we focus only on the users connected to the central HAPS. The users are dropped uniformly in a circle with a $2R$ km radius surrounding the central HAPS area, and they are connected to the cell with the maximum received power. The number of users connected to the central HAPS is at least 20,000.

The major parameters of the evaluation are summarized in Table 2, and explained in Section III-C. The DL transmission power is a design parameter and is fixed in value for all cells. The DL transmission power is 43 dBm/cell in IV-B to IV-E. The DL transmission power can be reduced to decrease the power consumption as long as the DL SNR constraints are satisfied. In the DL SINR calculation, we assume an activation factor β of 0.5 in Eqn. 6, which means that

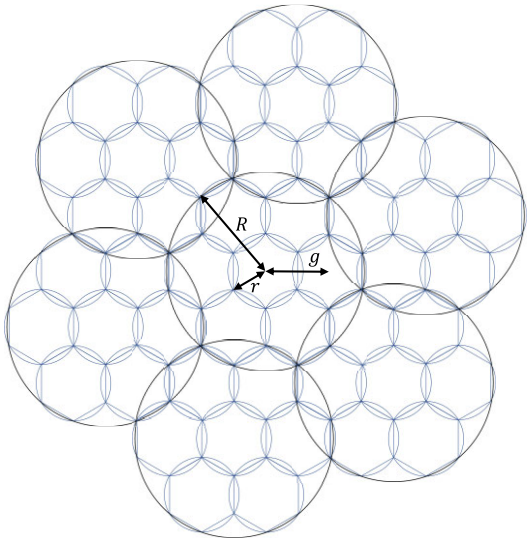

FIGURE 5. HAPS and cell geometry for hexagonal cell layout. (7 cells).

50% of the RBs are utilized in the neighbor cells for the interference calculation. Only in Section IV-D do the parameters take value every 1° to examine the beamwidth in detail.

B. PERFORMANCE EVALUATION

First, we show the performance gain of our proposed method. For comparison, we consider the geometrical approach presented in [10], where the antenna parameters were defined as the region bounded by the antenna half-power beamwidth contour. Fig. 5 shows a hexagonal cell layout, where each HAPS consists of 7 cells, to explain the following antenna beamwidth calculation. The vertical and horizontal beamwidths subtended by the circle of radius r are given by

$$\theta_{3\mathrm{dB}} = \arctan\left(\frac{g+r}{h}\right) - \arctan\left(\frac{g-r}{h}\right) \tag{14}$$

and

$$\phi_{3\mathrm{dB}} = 2\arctan\left(\frac{r}{\sqrt{g^2+h^2}}\right) \tag{15}$$

where g and h are the distance between the center of the HAPS and the center of each cell, and the height of the HAPS. The antenna tilt angle is given by

$$\theta_{\mathrm{tilt}} = \arctan\frac{h}{g} \tag{16}$$

Note that this geometrical approach can be defined for cell configurations with a single cell in the first layer, such as $(1, N-1)$ and $(1, M, N-M-1)$ configurations.

Fig. 6 compares the spectral efficiency at the median value between the proposed method and the geometrical approach for 7 cells with a (1,6) configuration and 19 cells with a (1, 6, 12) configuration. Fig. 7 compares the 1st-percentile values of the UL SNR under the same condition as that in Fig. 6.

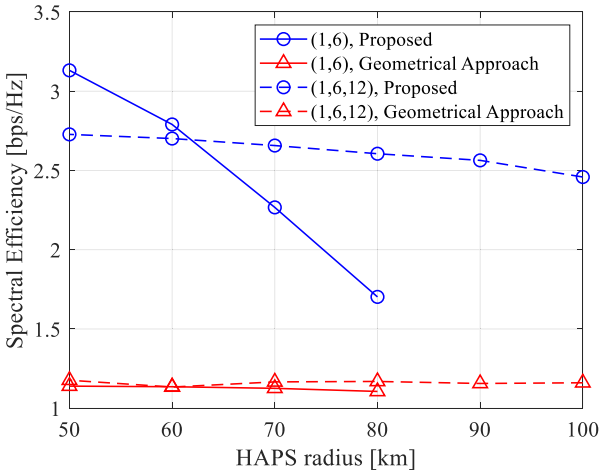

FIGURE 6. Comparison of spectral efficiency between proposed method and geometrical approach.

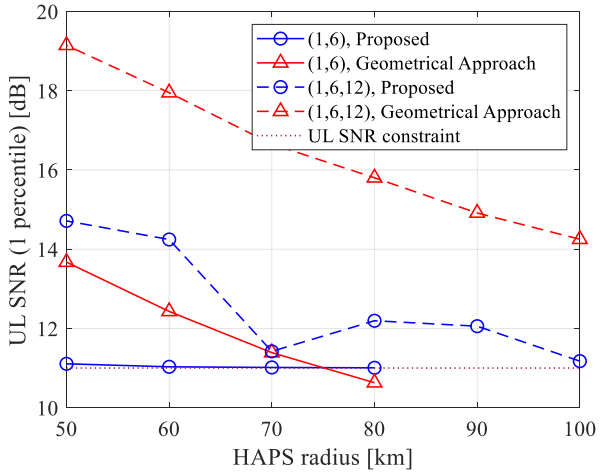

FIGURE 7. Comparison of 1st percentile uplink SNR between proposed method and geometrical approach.

In Fig. 6, the spectral efficiency of the proposed method is larger than that of the geometrical approach. By contrast, the UL SNR of the geometrical approach is larger than that of the proposed method for 50 km to 70 km with 7 cells, and for 50 km to 100 km with 19 cells. The beamwidth of the geometrical approach becomes wider than it needs to be in terms of constraints. On the contrary, the proposed method can narrow the beamwidth considering the constraints. For example, the vertical beamwidths of the (1,6) configuration in the second layer for the proposed method and the geometrical approach are 17° and 34°, respectively.

As for coverage condition, for 7 cells with the geometrical approach, the UL SNR is below the constraint level of 11 dB at 80 km, which means the geometrical approach cannot meet the coverage condition at this point. Furthermore, the spectral efficiency of the geometrical approach is almost the same for all distance ranges while the UL SNR enlarges as the HAPS radius decreases. In this sense, the geometrical approach is not suitable for enhancing the throughput performance because it does not take capacity into consideration for parameter calculation.

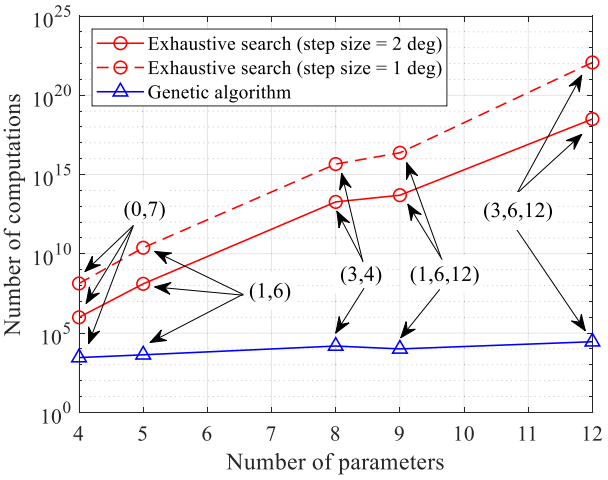

FIGURE 8. Number of parameters versus number of computations (50km).

C. COMPUTATIONAL COMPLEXITY AND OPTIMALITY OF RESULT

In this sub-section, we show the effectiveness of using the GA in terms of computational complexity. The number of computations grows greatly as the number of parameters, such as beamwidth and antenna tilt angle (Table 1), increases for exhaustive search. In Fig. 8, the total number of computations is shown for different numbers of parameters for both exhaustive search and GA. For example, we consider (0,7), (1,6), and (3,4) configurations for 7 cells; (1, 6, 12) configuration for 19 cells, and (3,6,12) configuration for 21 cells; the number of parameters is based on Table 1. The number of computations for the exhaustive search is derived from Table 3 for step sizes of 1° and 2°, where we assume a HAPS radius of 50 km as an example. The number of computations for GA is based on our evaluation, and it is the total number of generations multiplied by the population size. Thus, it may slightly differ depending on the randomness of the GA for different trials. Furthermore, the number of generations for convergence will generally increase as the population size decreases despite a reduction in the number of computations per generation. Reducing the population size will also increase the probability of falling into a local optimal solution.

The number of computations with 12 parameters exceeds 10^{18} for the step size of 2° and 10^{22} for the step size of 1°; therefore, it is virtually impossible to find an optimal combination by the exhaustive search. Nevertheless, the number of computations is largely reduced with the GA. The number of combinations for 12 parameters with the GA is reduced to below 10^5 despite the large number of parameters.

Secondly, we investigate the optimality of the GA result. We compare the results of the exhaustive search and the GA. We only investigate a case with 7 cells and a (1,6) configuration because exhaustive search is impossible for larger numbers of cells. The optimality is evaluated by how close the result of the GA is, compared with the optimal result of the exhaustive search; that is, the optimality is calculated by dividing the median spectral efficiency of the GA by that of the exhaustive search. Fig. 9 represents the spectral

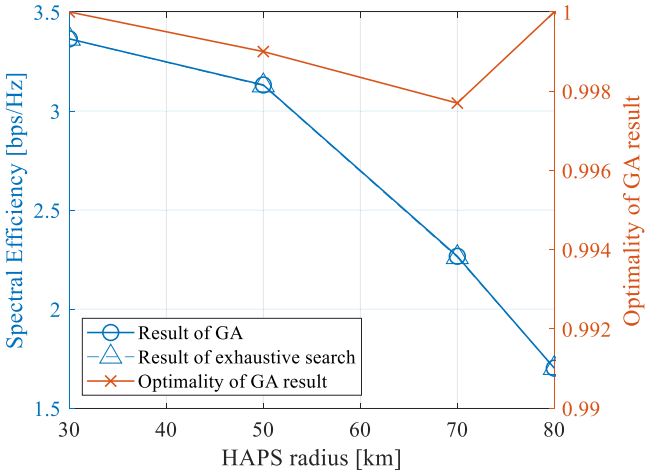

FIGURE 9. Optimality of the result of GA for the (1,6) configuration.

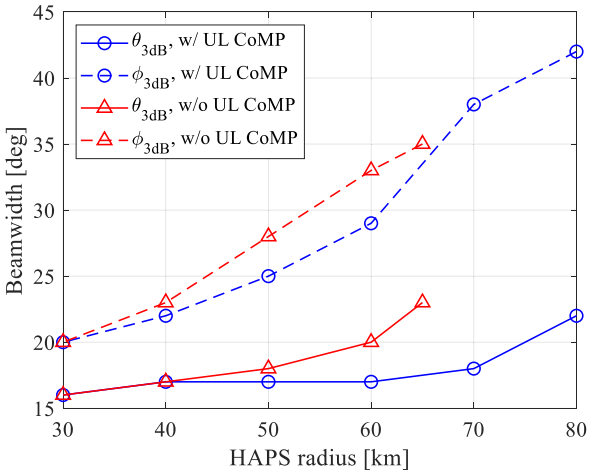

FIGURE 11. Vertical and horizontal beamwidth for 7 cells.

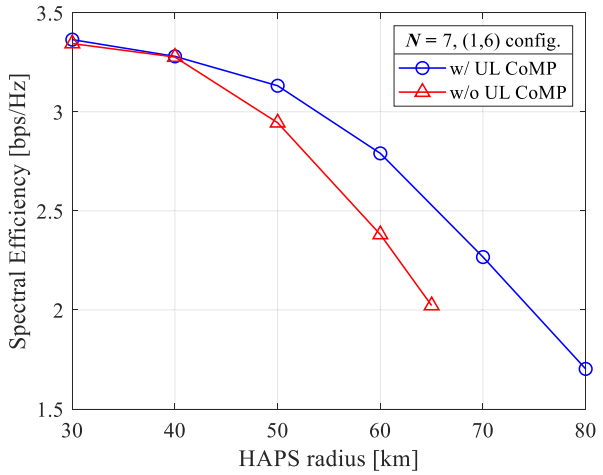

FIGURE 10. DL spectral efficiency for 7 cells configuration.

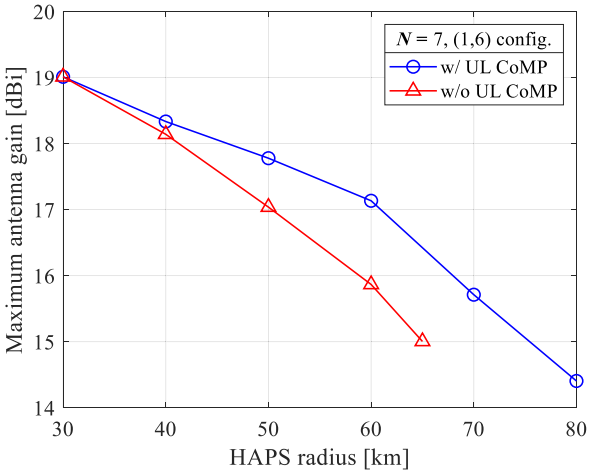

FIGURE 12. Maximum antenna gains for 7 cells.

efficiency of GA and the exhaustive search along with the optimality of results of the GA with the (1,6) configuration for different HAPS radii, which show that the result of GA is very close to that of the exhaustive search. The optimality for 30km and 80 km is 1.0000, which means the result of the GA exactly coincides with that of the exhaustive search. For 50 km and 70 km, the optimality is 0.9990 and 0.9977, which is also close to the result of the exhaustive search. Although GA is a meta-heuristic algorithm used to find sub-optimal results, the obtained results for the (1,6) configuration by the GA are very close to the optimal results of the exhaustive search, which can be concluded that the GA can be a good solution for finding good combinations while reducing the computational complexity.

D. EFFECT OF UL CoMP

As mentioned in Section III-C, UL CoMP can be a good solution for improving the UL SNR and extending the coverage area. First, we analyze the effectiveness of using UL CoMP. Fig. 10 compares the 50% median value of the DL spectral efficiency in a HAPS area with/without UL CoMP. We use a (1,6) configuration as an example. The DL spectral efficiency with/without UL CoMP is almost the same at 30 km to 40 km, and the difference gradually grows as the HAPS radius increases. The maximum HAPS radii are 80 km (with UL CoMP) and 65 km (without UL CoMP), which shows the effectiveness of UL CoMP for coverage extension.

Next, we examine why UL CoMP is effective for coverage extension. Fig. 11 shows the vertical and horizontal beamwidths with/without UL CoMP, and Fig. 12 shows the maximum antenna gains with/without UL CoMP. Fig. 11 indicates that the horizontal beamwidth without UL CoMP, ϕ_{3dB}, is slightly larger than that with UL CoMP, and the vertical beamwidth without UL CoMP, θ_{3dB}, becomes clearly larger than that with UL CoMP at more than 50 km. Correspondingly, the difference in antenna gain between with/without UL CoMP grows as the HAPS radius increases, as shown in Fig. 12. For smaller coverage, UL CoMP is not effective because enough antenna gain is sustained without UL CoMP. For larger coverage, UL CoMP effectively suppresses any increase in beamwidth while keeping the antenna gain as high as possible. There is no room for extending the beamwidth at more than 65 km without UL CoMP because the UL SNR constraint will not be satisfied.

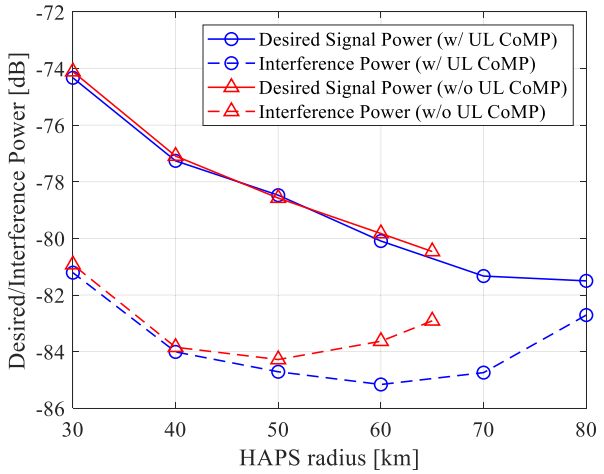

FIGURE 13. Desired signal power and interference for 7 cells.

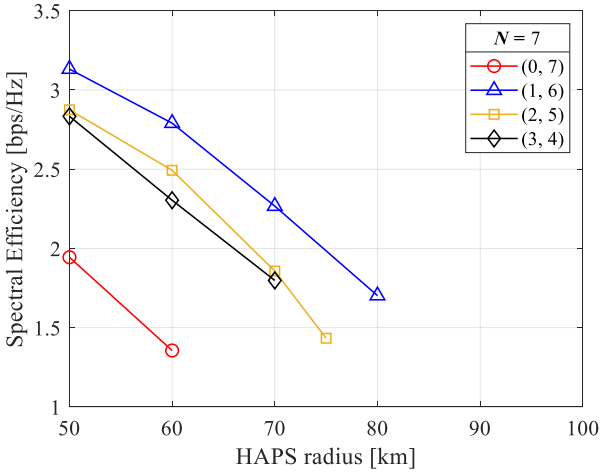

FIGURE 14. DL spectral efficiency of different cell configuration (7 cells).

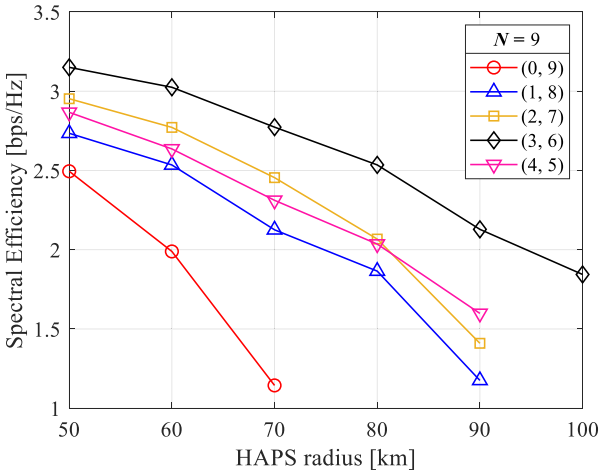

FIGURE 15. DL spectral efficiency of different cell configuration (9 cells).

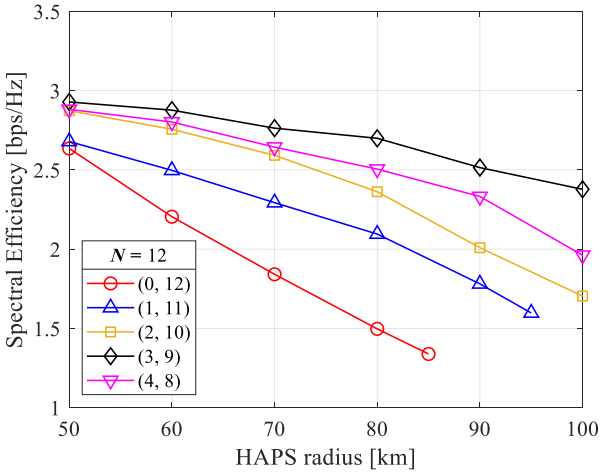

FIGURE 16. DL spectral efficiency of different cell configuration (12 cells).

Even if a wide area is covered by a HAPS, degradation in spectral efficiency is unavoidable. Covering a wider area requires a broader beamwidth as shown in Fig. 11. With a broader beamwidth, the antenna gain (or desired signal power) will decrease, and interference will increase. Fig. 13 shows the desired signal power and interference power with/without UL CoMP when we assume a full buffer. The figure indicates that the desired signal power decreases as the HAPS radius increases. Although interference decreases up to 50 km without UL CoMP and up to 60 km with UL CoMP, interference increases after these. Therefore, both the decrease in desired signal power and increase in interference power are attributed to the degradation of the DL SINR, namely, spectral efficiency. Furthermore, the interference without UL CoMP is much larger than that with UL CoMP at 65 km, which shows the effectiveness of UL CoMP in reducing interference by keeping the beamwidth narrow.

E. OPTIMAL CELL CONFIGURATIONS

Next, we clarify the optimal cell configuration according to the number of cells. Figs. 14–18 show the 50% median value of the DL spectral efficiency of different cell configurations for 7, 9, 12, 19, and 21 cells. We compare the $(0, N)$ and $(M, N-M)$ configurations for 7–12 cells, where M is 1, 2, and 3 for the 7 cells; M is 1, 2, 3, and 4 for 9 and 12 cells. For the 19 cells, M is 5, 6, and 7 for the $(M, N-M)$ configuration. For the 21 cells, M is 6, 7, and 8 for the $(M, N-M)$ configuration. In addition, as this is a three-layer configuration, we assume a $(1, M, N-M-1)$ configuration for 19 cells and $(3, M, N-M-1)$ for 21 cells, where M is 5, 6, and 7.

According to Figs. 14–18, the optimal cell configuration is $(M, N-M)$, where $M = 1$, for the 7 cells; $(M, N-M)$, where $M = 3$, for the 9 and 12 cells; $(1, M, N-M-1)$ where $M = 6$, for the 19 cells; and $(3, M, N-M-1)$, where $M = 6$, for the 21 cells. Thus, the optimal cell configuration depends on the number of cells. Moreover, the $(0, N)$ configuration has limited coverage compared with the other configurations for the 7 to 12 cells; this finding highlights the importance of placing a cell in the central area when the number of cells is limited.

For example, a vertical beamwidth, $\theta_{3\text{dB}}$, of the (0,7) configuration at 60 km is 46°, and that of the (1,6) configuration is 16°; these are because a single layer must cover from the

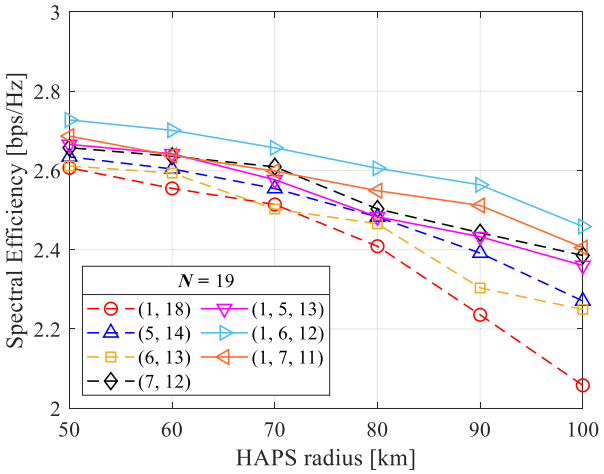

FIGURE 17. DL spectral efficiency of different cell configuration (19 cells).

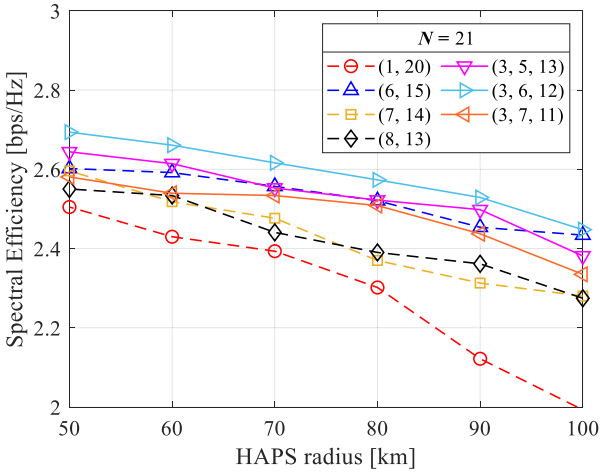

FIGURE 18. DL Spectral efficiency of different cell configuration (21 cells).

center to the cell edge with a wide beamwidth. The (1,6) configuration can narrow the vertical beamwidth because the central area is covered by the central cell, thereby effectively keeping antenna gain of the second layer high due to the narrow beamwidth.

Fig. 19 compares the optimal cell configurations of the different numbers of cells. The best cell configuration in terms of the 50% median value of spectral efficiency is (3,6) between 50 km and 70 km, (3,9) at 80 km, and (1,6,12) from 90 km. One reason why the cell configuration of the 12, 19, and 21 cells has a lower spectral efficiency than that for the 7 and 9 cells at 50 km is the amount of interference from other cells and HAPSs. With the same number of HAPSs, interference increases with the number of cells. The interference power for the 50% median user at 50 km is −84.71 dBm, −85.79 dBm, −80.03 dBm, −79.32 dBm, and −69.46 dBm for the 7, 9, 12, 19, and 21 cells, respectively, showing that the interference of 7 and 9 cells is smaller than those of the others. Although the desired signal power also increases as a result of the higher antenna gain for a large number of cells, interference occurs because many cells squeeze into a smaller area, resulting in low spectral efficiency.

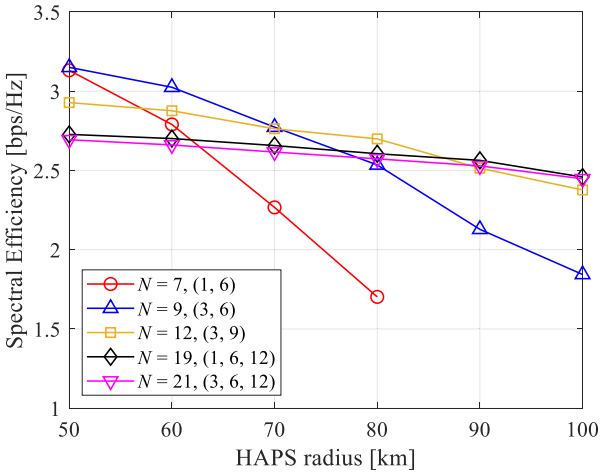

FIGURE 19. Comparison of DL spectral efficiency of optimal cell configurations.

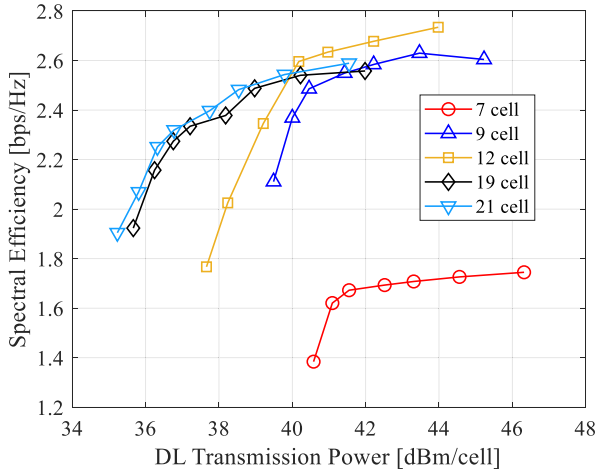

FIGURE 20. DL Spectral efficiency versus DL transmission power per cell (80 km).

F. ANALYSIS OF ENERGY EFFICIENCY

We have discussed the type of cell configuration that is the best according to the number of cells. It is important to investigate power consumption reduction from the viewpoint of practical implementation because the acceptable power consumption on HAPSs is usually limited.

In this sub-section, we assume the cell configurations that are proved to be optimal in the previous sub-section, that is, (1,6) for 7 cells, (3,6) for 9 cells, (3,9) for 12 cells, (1,6,12) for 19 cells, and (3,6,12) for 21 cells.

Fig. 20 shows the 50% median value of spectral efficiency for different transmission power per cell when the HAPS radius is 80 km. The DL transmission power is reduced, and the DL SNR constraint is eventually not satisfied. With focus on the 7 cells, the spectral efficiency is apparently lower than that of the other numbers of cells. This result is consistent with the fact that covering a wide area with a small number of cells decreases the antenna gain with a broader beamwidth. Moreover, the spectral efficiency is stable from 46 dBm/cell to around 42 dBm/cell, but it drops

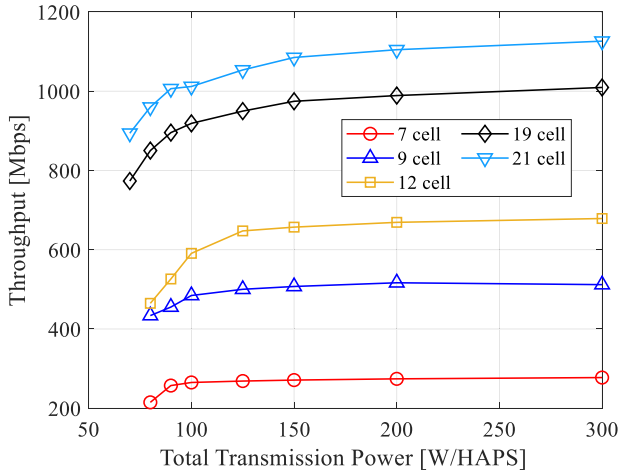

FIGURE 21. DL throughput versus total transmission power (80 km).

rapidly afterward. This trend occurs because the beamwidth enlarges to meet the DL SNR constraint and thus compensate for the decrease in DL transmission power. The optimal parameters are completely the same between 46.32 dBm/cell and 41.55 dBm/cell, and the beamwidth increases to satisfy the SNR constraints until the constraints are not satisfied below 41.55 dBm/cell. This tendency can also be seen in the other cell configurations. The minimum transmission power per cell becomes small as the number of cells becomes large. When we assume the same HAPS radius, the area covered by a cell can be reduced by increasing the number of cells, which leads to a higher antenna gain, effectively reducing the DL transmission power. For example, the spectral efficiency of the 21 cells with 43 dBm/cell is 2.57 bps/Hz. If a 10% decrease in spectral efficiency is permitted, then the transmission power can be reduced by 6.22 dBm/cell to 36.78 dBm/cell. Furthermore, the spectral efficiency of the 12 cells at 43 dBm/cell is 2.7 bps/Hz. Similarly, the DL transmission power can be reduced by 3.5 dBm/cell to around 39.5 dBm/cell. Therefore, increasing the number of cells effectively realizes energy-efficient HAPS mobile communications.

Fig. 21 represents the throughput for different total transmission power given a HAPS radius of 80 km. Please note that the throughput is calculated based on the Shannon capacity with the activation factor of 0.5 assuming RBs are equally allocated to all UEs. With a certain total transmission power constraint, increasing the cells can enhance the throughput without increasing the total transmission power for the same coverage area. Notably, 21 and 19 cells can achieve gigabit throughput. Thus, a multi-layer cell configuration with a large number of cells is crucial for achieving high capacity mobile communications.

The throughput of the 7 cells with 300 W is 277 Mbps, and that of the 21 cells with 300 W is about 1.1 Gbps, which means three-fold the number of cells can achieve more than a three-fold throughput. Moreover, the 21 cells can keep 1 Gbps reducing the total transmission power to 90 W per HAPS. Thus, it is important to implement as many cells as a UAV can accommodate to be energy-efficient.

V. CONCLUSION

In this paper, we propose an optimization method for cell configurations in HAPS mobile communications. The number of cells a HAPS can accommodate varies depending on UAV ability. By contrast, optimal cell configurations for arbitrary numbers of cells had not been investigated. Our proposed method employs a GA to optimize multiple parameters required to form a cell configuration in a practical time, given that the combination of multiple parameters enlarges as the cell configuration become increasingly complex. We clarify optimal cell configurations for different numbers of cells and show that the optimal configuration depends on the number of cells. We also show that our proposed method outperforms simple geometrical approach in terms of spectral efficiency.

Considering the spread of mobile broadband communications in recent years, researchers expect to improve capacity through HAPSs. Although multi-cell configurations are essential for realizing gigabit HAPS mobile communications, increasing the number of cells is a critical problem due to the limitation of power consumption. Thus, we also investigate energy efficiency. We demonstrate that multi-layer cell configurations with large numbers of cells are desirable for realizing gigabit HAPS mobile communications, and installing as many cells as possible is effective in terms of both capacity and energy efficiency.

REFERENCES

[1] S. Karapantazis and F. Pavlidou, "Broadband communications via high-altitude platforms: A survey," *IEEE Commun. Surveys Tuts.*, vol. 7, no. 1, pp. 2–31, 1st Quart., 2005.

[2] R. Miura and M. Oodo, "Wireless communications system using stratospheric platforms: R and D program on telecom and broadcasting system using high altitude platform stations," *J. Commun. Res. Lab.*, vol. 48, no. 4, pp. 33–48, Dec. 2001.

[3] S. A. R. Naqvi, S. A. Hassan, H. Pervaiz, and Q. Ni, "Drone-aided communication as a key enabler for 5G and resilient public safety networks," *IEEE Commun. Mag.*, vol. 56, no. 1, pp. 36–42, Jan. 2018.

[4] K. Hoshino, S. Sudo, and Y. Ohta, "A study on antenna beamforming method considering movement of solar plane in HAPS system," in *Proc. IEEE 90th Veh. Technol. Conf. (VTC-Fall)*, Hawaii, HI, USA, Sep. 2019, pp. 1–5.

[5] Y. Shibata, N. Kanazawa, K. Hoshino, Y. Ohta, and A. Nagate, "A study on cell configuration for HAPS mobile communications," in *Proc. IEEE 89th Veh. Technol. Conf.*, Kuala Lumpur, Malaysia, Apr. 2019, pp. 1–6.

[6] (Aug. 2018). *Airbus Zephyr Solar High Altitude Pseudo-Satellite flies for Longer Than any Other Aircraft During its Successful Maiden Flight* [Online]. Available: https://www.airbus.com/newsroom/press-releases/en/2018/08/Airbus-Zephyr-Solar-High-Altitude-Pseudo-Satellite-flies-for-longer-than-any-other-aircraft.html.

[7] D. Yuniarti, "Regulatory challenges of broadband communication services from high altitude platforms (HAPs)," in *Proc. Int. Conf. Inf. Commun. Technol. (ICOIACT)*, Yogyakarta, Mar. 2018, pp. 1–5.

[8] F. A. D'Oliveira, F. C. L. D. Melo, and T. C. Devezas, "High-altitude Platforms–Present situation and technology trends," *J. Aerosp. Technol. Manage.*, vol. 8, no. 3, pp. 249–262, Aug. 2016.

[9] *HAPSMobile Successfully Completes Latest Test Flight of its Unmanned Aircraft Designed for Stratospheric Telecommunications Platform Systems*. Accessed: Jul. 30, 2020. [Online]. Available: https://www.hapsmobile.com/en/news/press/2020/20200730_01/

[10] J. Thornton, D. Grace, M. H. Capstick, and T. C. Tozer, "Optimizing an array of antennas for cellular coverage from a high altitude platform," *IEEE Trans. Wireless Commun.*, vol. 2, no. 3, pp. 484–492, May 2003.

[11] S. H. Alsamhi and N. S. Rajput, "HAP antenna radiation pattern for providing coverage and service characteristics," in *Proc. Int. Conf. Adv. Comput., Commun. Inform. (ICACCI)*, New Delhi, India, 2014, pp. 1–5.

[12] Iskandart, S. Gratsia, and M. E. Ernawan, "LTE uplink cellular capacity analysis in a high altitude platforms (HAPS) communication," in *Proc. 11th Int. Conf. Telecommun. Syst. Services Appl. (TSSA)*, Lombok, U.K., Oct. 2017, pp. 1–5.
[13] Z. Yang, A. Mohammed, and T. Hult, "Uplink performance evaluation of WiMAX broadband services via high altitude platforms (HAPs)," in *Proc. 2nd Eur. Conf. Antennas Propag. (EuCAP)*, Edinburgh, U.K., 2007, pp. 1–8.
[14] K. G. Siahaan and Iskandar, "Performance improvement on the downlink HAPS communication channel employing MIMO antenna," in *Proc. 10th Int. Conf. Telecommun. Syst. Services Appl. (TSSA)*, Denpasar, Germany, Oct. 2016, pp. 1–8.
[15] D. Grace and M. Mihael, *Broadband Communications Via High-Altitude Platforms*. Hoboken, NJ, USA: Wiley, 2011.
[16] *Minimum Performance Characteristics and Operational Conditions For High Altitude Platform Stations Providing IMT-2000 in the Bands 1885-1980 MHz, 2010-2 025MHz and 2110-2170 MHz in Regions 1 and 3 and 1885- 1980 MHz and 2110-2160 MHz in Region 2*, document ITU-R M.1456, 2000.
[17] C. Queiroz, R. Vieira, A. Barreto, A. Zarrebini, E. Souza, and A. Linhares, "New spectrum bands for HAPS: Sharing with fixed-satellite systems," in *Proc. IEEE 89th Veh. Technol. Conf. (VTC-Spring)*, Kuala Lumpur, Malaysia, Apr. 2019, pp. 1–5.
[18] *Characteristics of Terrestrial IMT-Advanced Systems for Frequency Sharing/Interference Analyses*, document ITU-R M.2292-0, 2013.
[19] L. Falconetti and S. Landstrom, "Uplink coordinated multi-point reception in LTE heterogeneous networks," in *Proc. 8th Int. Symp. Wireless Commun. Syst.*, Nov. 2011, pp. 1–5.
[20] K. Deb, "An efficient constraint handling method for genetic algorithms," *Comput. Methods Appl. Mech. Eng.*, vol. 186, nos. 2–4, pp. 311–338, Jun. 2000.

YOHEI SHIBATA received the B.E. and M.E. degrees from Keio University, Japan, in 2014 and 2016, respectively. He joined SoftBank Corporation, Tokyo, Japan, as a Research Engineer, in 2016. He is a member of IEICE.

NOBORU KANAZAWA received the B.E. and M.E. degrees from the University of Tokyo, Japan, in 2012 and 2014, respectively. He joined SoftBank Corporation, Japan, as a Research Engineer, in 2014.

MITSUKUNI KONISHI received the M.E. degree from the Tokyo University of Science, in 2013. He joined SoftBank Mobile Corporation (currently, SoftBank Corporation), in 2013. He has also been a Research Engineer with the Technology Research Laboratory, SoftBank Corporation.

KENJI HOSHINO received the M.E. degree in information engineering from the Shibaura Institute of Technology, in 2007. He joined Softbank Telecom Corporation (currently, SoftBank Corporation), in 2007. He has also been a Research Engineer with the Research and Development, SoftBank Corporation. He received the Academic Encouragement Award from IEICE, in 2012. He is a member of IEICE.

YOSHICHIKA OHTA received the B.E. and M.E. degrees from the Muroran Institute of Technology, Japan, in 2000 and 2002, respectively. He joined Japan Telecom Company Ltd., (currently, SoftBank Corporation), Tokyo, Japan, in 2002. He is currently a Manager of Wireless System Research and Development Section, Technology Research Laboratory, SoftBank Corporation. He is also a Manager of Wireless System Research and Development Section, Research and Development Department, HAPSMobile Inc., Tokyo. His current research interests include RF and wireless communication devices and systems, smart antenna systems, and SDR systems.

ATSUSHI NAGATE (Member, IEEE) received the M.E. and Ph.D. degrees from Osaka University, in 2001 and 2016, respectively. He joined Japan Telecom Company Ltd., (currently, SoftBank Corporation), in 2001, where he has been engaged in research and development of mobile communication systems. He is currently the Director of the Technology Research Laboratory, SoftBank Corporation. He is also the Director of the Research and Development Department, HAPSMobile Inc. His research interests include mobile communications and UAV communications. He is a member of IEICE.